

ACTIVATION OF TRANSIENT RECEPTOR POTENTIAL VANILLOID 3 REGULATES INFLAMMATORY ACTIONS OF HUMAN EPIDERMAL KERATINOCYTES

Attila Gábor Szöllösi^{1,*}, Nikolett Vasas^{1,*}, Ágnes Angyal¹, Kornél Kistamás¹, Péter Pál Nánási¹, Johanna Mihály², Gabriella Béke³, Erika Herczeg-Lisztes¹, Andrea Szegedi³, Naoki Kawada⁴, Takashi Yanagida⁴, Takahiro Mori⁴, Lajos Kemény⁵, Tamás Bíró^{1,2}

¹Department of Physiology, Faculty of Medicine, University of Debrecen, Debrecen, Hungary

² Department of Immunology, Faculty of Medicine, University of Debrecen, Debrecen, Hungary

³ Department of Dermatology, Faculty of Medicine, University of Debrecen

⁴ Exploratory Research Laboratories II, Ono Pharmaceutical Co., Ltd.

⁵ Department of Dermatology and Allergology, University of Szeged, Szeged, Hungary

* Authors contributed equally to this work

This work was performed in Debrecen, Hajdú-Bihar, Hungary

Correspondence should be addressed to:

Attila Gábor Szöllösi

Department of Physiology, University of Debrecen, Faculty of Medicine H-4002
DEBRECEN Nagyerdei krt. 98. PO BOX 400. HUNGARY

Office Phone: +36-52-255-575/55378

FAX: +36-52-255-116

Email: szollosi.attila@med.unideb.hu

Short title: TRPV3 regulates inflammation of keratinocytes

Keywords: transient receptor potential vanilloid, keratinocyte, inflammation, nuclear factor kappa-light-chain-enhancer of activated B cells

Abbreviations: 2-APB, 2-aminoethoxydiphenyl-borate; IL, interleukin; IR, immunoreactivity; NC, negative control; NHEK, normal human cultured keratinocytes; $[Ca^{2+}]_{ic}$, intracellular calcium concentration; TNF- α , tumor necrosis factor alpha; TRP, transient receptor potential

ABSTRACT

Transient receptor potential (TRP) ion channels were first characterized on neurons, where they are classically implicated in sensory functions; however, research in recent decades has shown that many of these channels are also expressed on non-neuronal cell types. Emerging findings have highlighted the role of TRP channels in the skin, where they have been shown to be important in numerous cutaneous functions. Of particular interest is TRPV3, which was first described on keratinocytes. Its functional importance was supported when its gain-of-function mutation was linked to Olmsted syndrome, which is characterized by palmoplantar keratoderma, periorifacial hyperkeratosis, diffuse hypotrichosis and alopecia, as well as itch. In spite of these exciting results, we have no information about the role and functionality of TRPV3 on keratinocytes at the cellular level. In our current study, we have identified TRPV3 expression both on human skin and cultured epidermal keratinocytes. TRPV3 stimulation was found to function as a Ca^{2+} -permeable ion channel which suppresses proliferation of epidermal keratinocytes and induces cell death. Stimulation of the channel also triggers a strong proinflammatory response via the NF- κ B pathway. Collectively our data shows that TRPV3 is functionally expressed on human epidermal keratinocytes and that it plays a role in cutaneous inflammatory processes.

INTRODUCTION

The 27 cation channels that compose the transient receptor potential (TRP) ion channel superfamily in humans respond to a remarkably diverse variety of chemical and physical stimuli (Nilius and Owsianik 2011; Wu et al. 2010). An interesting subset of these cellular sensors are activated by changes in temperature, and are therefore classified as thermo-TRPs. This subset encompasses a total of ten channels, which are members of the vanilloid (TRPV1, TRPV2, TRPV3 and TRPV4), ankyrin (TRPA1), and melastatin (TRPM2, TRPM3, TRPM4, TRPM5 and TRPM8) subfamilies of TRP channels (Oberwinkler and Philipp 2014; Saito and Shingai 2006; Vay et al. 2012). Of note, these channels not only respond to discreet, at times overlapping temperature ranges but many of them are activated by pungent compounds found in common spices (e.g. capsaicin from chili peppers activates TRPV1, allicin from garlic activates TRPV1 and TRPA1, while eugenol from cloves, carvacrol from oregano, thymol from thyme all activate TRPV3) (Nilius and Appendino 2013). Although most TRP channels were first characterized on neurons, where they are classically implicated in sensory functions (pain, itch, thermal hyperalgesia, thermosensation, mechanosensation), research in recent decades has shown that many of these channels are also expressed on non-neuronal cell types (Fernandes et al. 2012). Of particular interest is the role of TRP channels in the skin, where they have been shown to be important in epidermal barrier formation and maintenance (TRPV1 [(Denda et al. 2007; Tóth et al. 2011)], 3 [(Cheng et al. 2010; Denda et al. 2007)], 4 [(Denda et al. 2007)], 6 [(Lehen'kyi et al. 2011; Lehen'kyi et al. 2007)] and TRPM8 [(Denda et al. 2010)], TRPA1[(Atoyán et al. 2009)], the regulation of the hair cycle (TRPV1 [(Bodó et al. 2005)] and 3 [(Borbiró et al. 2011)]), melanogenesis (TRPM1 [(Devi et al. 2009; Oancea et al. 2009)]) and tumor progression (TRPC1 and 4 [(Beck et al. 2008)]).

Interestingly, while most TRP channels were first described on neurons, TRPV3, a sensor of innocuous warm temperatures (31-39 °C), was first described in keratinocytes (Peier et al.

2002). TRPV3 is a 6 transmembrane protein that forms non-selective cation channels mainly permeable to calcium as homo- or heterotetramers and is 43% homologous with TRPV1. TRPV3 is also activated by the aforementioned plant-derived compounds, as well as the synthetic agonist 2-aminoethoxydiphenyl-borate (2-APB) (Chung et al. 2004a; Xu et al. 2006).

The physiological relevance of TRPV3 expression in the skin was highlighted when the hairless DS-Nh mouse strain was linked to a gain-of-function mutation in the *TRPV3* gene caused by a Gly573Ser mutation in keratinocytes (Asakawa et al. 2006). This mutation led to not only hairlessness but also to the development of spontaneous dermatitis and pruritus, increased *Staphylococcus aureus* colonization, higher IgE and IL-4 levels, increased CD4+ T-cell infiltration, and hyperkeratosis in the affected mice, hinting at the potentially complex role of TRPV3 in cutaneous pathophysiology (Yoshioka et al. 2009).

Further underlining the human relevance of these results the same Gly573Ser mutation was found in a very rare disorder in humans, Olmsted syndrome. Symptoms of the condition include palmoplantar keratoderma, periorifacial hyperkeratosis, diffuse hypotrichosis and alopecia, and itch. Concomitant histological findings include hyperkeratosis, parakeratosis and psoriasiform lesions, with mast cell infiltration in the upper part of the dermis, which coincides with the murine data mentioned above (Lin et al. 2012). The functional relevance of this channel is further highlighted by a search of the GEO Profiles database (Barrett et al. 2013) which shows that the level of TRPV3 expression is higher in psoriasis, a common inflammatory skin disease (GEO ascension GDS4602) (Nair et al. 2009). TRPV3 expression was also shown to be increased in papulopustular rosacea and erythematotelangiectic rosacea (Sulk et al. 2012).

In line with these results our workgroup has previously investigated the role of TRPV3 on hair follicles and outer root sheath keratinocytes (Borbíró et al. 2011). Based on these previous results TRPV3 is not only functionally expressed, but its activation inhibits hair growth and cellular proliferation and induces cell death on these cells.

In the current study we aimed at characterizing the native role of TRPV3 on normal human keratinocytes, to elucidate the role of the channel on the most abundant cell type of the skin on a cellular level.

RESULTS

Human skin and cultured human epidermal keratinocytes express TRPV3

First, we intended to define TRPV3 expression in the human skin, using full-thickness normal skin obtained from healthy individuals by punch biopsy. As revealed by immunohistochemistry, TRPV3 was identified the outermost layer of the skin, the epidermis (Figure 1a). TRPV3-immunoreactivity (IR) showed a homogenous staining between the stratum basale and stratum corneum. In good accord with these data, a strong TRPV3-IR was observed on normal human cultured keratinocytes (NHEKs), both by immunocytochemistry (Figure 1c) and Western blotting (Figure 1e) in both preconfluent (80%) and postconfluent (PC2) cells. The specificity of the immunosignal was assessed by appropriate negative controls (Figure 1b and d) (see also Materials and Methods section for details).

This corresponded well to expression of the TRPV3 gene in human tissue and NHEKs, as demonstrated by quantitative real-time PCR. As shown in Figure 1f, mRNA transcripts for TRPV3 were unambiguously identified in normal human skin, as well as in pre- and post-confluent cultured epidermal keratinocytes.

TRPV3 is expressed as a Ca²⁺-permeable ion channel on NHEKs

Next, we studied the functionality of TRPV3 channel in a series of dynamic imaging and electrophysiological experiments, performed on NHEKs. Using whole-cell patch-clamp configurations, membrane currents were elicited by voltage-ramp protocols (Figure 2a and b). Control NHEKs showed outwardly rectifying currents with an average reversal potential of -46.1 ± 1 mV (mean \pm SEM, n=6). Then currents were normalized to cell membrane capacitance at four different potentials, i.e., at -90, -40, +40, and +90 mV resulting -3.6 ± 1.1 , -0.4 ± 0.1 , 3.5 ± 0.5 , and 8.2 ± 1.4 pA/pF, respectively (all data are mean \pm SEM values) (Figure 2c).

Of great importance, both inward and outward currents were markedly and significantly ($P < 0.05$) increased by 100 μ M carvacrol (Figure 2a-c), a TRPV3 agonist, which effect was found to be reversible by thorough washout. In the presence of carvacrol, the currents measured at -90, -40, +40, and +90 mV were -7.2 ± 2.3 , -2.4 ± 1.0 , $+5.4 \pm 1.0$, and $+14.5 \pm 3.0$ pA/pF, respectively (mean \pm SEM, $n=6$).

To further support the functionality of TRPV3, we took advantage of the well-known fact that TRPV3 (similarly to the majority of the TRP channels) operates as a mostly (but not exclusively) calcium permeable ion channel (Moran et al. 2011). Using a fluorescent Ca^{2+} -measurement technique, we found that TRPV3 agonists significantly increased the intracellular calcium concentration ($[\text{Ca}^{2+}]_{\text{ic}}$) in a dose-dependent manner (Figure 2d-f). Of further importance, the actions of the TRPV3 agonists to elevate $[\text{Ca}^{2+}]_{\text{ic}}$ was abrogated in nominally calcium-free extracellular medium (from 1.8 to 0.02 mM) (Figure 2f), suggesting that these agents indeed opened surface membrane Ca^{2+} -permeable channels of the NHEKs. Supporting these findings we have also shown that RNAi mediated knock-down of TRPV3 significantly reduces the calcium signal elicited by carvacrol (Supplementary Figure 2).

Cellular physiology data and Ca^{2+} -measurement data collectively argued for the fact that NHEKs indeed express functional TRPV3, which operates as a nonselective cation channel at the plasma membrane of the cells that are most permeable to Ca^{2+} , similar to that previously described for human outer root sheath keratinocytes and murine epidermal keratinocyte populations (Borbíró et al. 2011; Cheng et al. 2010; Chung et al. 2004a; Chung et al. 2004b; Huang et al. 2008; Peier et al. 2002).

TRPV3 stimulation suppresses proliferation of epidermal keratinocytes and induces cell death

We then investigated the cellular effects of TRPV3 activation on growth and survival of human epidermal keratinocytes. Cells were exposed to various TRPV3 agonists, such as carvacrol – a plant derived agent – and a synthetic agonist 2-aminoethoxydiphenyl borate (2-APB) (Chung et al. 2004b; Xu et al. 2006). We found that carvacrol and 2-APB dose-dependently reduced cell viability and proliferation of NHEK cells (Figure 3a and b).

Several lines of evidence suggest that the above agents may also activate other TRP channels (Bíró et al. 2007; Xu et al. 2006). Furthermore, we lack highly selective and commercially available TRPV3 antagonists. Therefore, the TRPV3 specificity of the effect of carvacrol and 2-APB was further assessed and verified by RNA interference. A series of TRPV3-targeted RNAi knockdown experiments were carried out in accordance with the techniques developed in our previous studies and which were optimized for various cultured human skin cells (Borbíró et al. 2011; Dobrosi et al. 2008; Oláh et al. 2014; Szöllösi et al. 2013; Tóth et al. 2009). Importantly, we found that successful silencing of TRPV3 (Supplementary Figure 1.) was able to almost completely prevent the aforementioned detrimental effects on the viability and proliferation (Figure 3a and b), indicating that TRPV3-mediated signaling indeed plays a crucial role in conducting cellular actions of these agents. We also determined the mechanism of these observed effects, by investigating the decrease of mitochondrial membrane potential (one of the earliest markers of apoptosis) and the membrane integrity (to rule out necrotic events). According to our data a high concentration of carvacrol (300 μ M) and 2-APB (100 μ M) both cause significant decrease of mitochondrial membrane potential (Supplementary Figure 3), while membrane integrity was not affected (Supplementary Figure 3). Based on these data we can assert that TRPV3 activation leads to apoptotic cell death. Interestingly the use of the calcium chelator ethylenediaminetetraacetic acid (EDTA) did not influence the observed effects (Supplementary Figure 4), which shows that this effect of carvacrol and 2-APB is not dependent on calcium mobilization from the extracellular space.

TRPV3 triggers strong proinflammatory response

As the 24 hr treatments were found to decrease proliferation and viability, we next investigated the cellular effects of TRPV3 activation in short-term experiments, by monitoring the expressional alterations of key pro-inflammatory cytokines (interleukin [IL]-1 α , IL-6, IL-8 and tumor necrosis factor [TNF]- α), since TRPV3 activation and gain-of-function mutation have been shown to result in marked cutaneous inflammation in both men and mice (Danso-Abeam et al. 2013; Yoshioka et al. 2009). We found that TRPV3 agonists significantly increased the expression of pro-inflammatory cytokines (Figure 4a and b) and also triggered a remarkable IL-6 and IL-8 release on the epidermal keratinocytes (Figure 4c and d). Importantly, we found that, similar to the above mentioned effects on the viability and proliferation, selective silencing of TRPV3 was able to almost completely abolish the up-regulation and release of the aforementioned cytokines (Figure 4a-d), indicating that pro-inflammatory actions of carvacrol and 2-APB were indeed mediated via the activation of TRPV3.

TRPV3-induced proinflammatory actions involve the NF- κ B pathway

Finally, we aimed at identifying the intracellular signaling pathway, which mediates the pro-inflammatory action of TRPV3 activation. It is well known, that activation of the NF- κ B pathway plays an important role in the regulation of inflammatory actions (Wullaert et al. 2011); hence, we investigated the involvement of this mechanism. We found that, 30 min carvacrol treatment induced the phosphorylation (and therefore inactivation) of the inhibitory I κ B α and phosphorylation (and therefore activation) of the p65 NF- κ B isoform. Both mentioned effects was abrogated by the co-application of EDTA (Figure 4e).

One of the hallmarks of NF- κ B activation is the translocation of p65 to the nucleus of the cell. To support our western blot data we also investigated this process on NHEK cells (Figure 4 f-

i). Compared to the control (Figure 4 f) 300 μ M of carvacrol caused significant increase in nuclear staining, comparable to that caused by the TLR-3 agonist polyinosinic:polycytidylic acid (poly I:C), a known inducer of NF- κ B translocation in keratinocytes (Takai et al. 2014). The full images the representative cells were cropped from, as well as the concurrent DAPI staining may be found in the supplementary material (Supplementary Figure 5).

Our previous findings show that TRPV3 is a functionally active calcium-permeable cation channel in keratinocytes; therefore, since the removal of extracellular calcium with EDTA abrogated the NF- κ B activation, it is likely that TRPV3 activation leads to the initiation of the aforementioned pathway. These findings collectively argued for the crucial involvement of the NF- κ B signaling pathway in mediating the inflammatory actions by TRPV3 activation in human epidermal keratinocytes.

Since the NF- κ B pathway is known to promote cell survival in keratinocytes (Qin et al. 1999), and our results showed that TRPV3 activation lead to decreased cell proliferation and viability (Figure 3 a and b), we wished to investigate the role of NF- κ B on these processes. To answer this question we tested whether the NF- κ B inhibitor BAY11-7085 would have any effect on our previous findings. As seen in Supplementary Figure 6, the use of the inhibitor in combination with the TRPV3 activator carvacrol further decreased the viability of the cells. This seems to show that TRPV3 activation activates more than one signaling pathway, and that the NFKB activation partially counteracts the negative effect of carvacrol on the cells' viability.

DISCUSSION

Recent research has shown that various mutations of the *TRPV3* gene are the underlying cause of both the phenotype of DS-Nh mice and for Olmsted syndrome, a serious cutaneous condition characterized by palmoplantar keratoderma, periorifacial hyperkeratosis, diffuse hypotrichosis and alopecia, and itch (Asakawa et al. 2006; Lin et al. 2012). Previous reports on TRPV3 have centered around observations in mice, where it has been described that: (i) the gain-of-function mutation of TRPV3 shows higher Ca^{2+} incorporation and NGF production as compared to DS mice without the mutation (Imura et al., 2007; Yoshioka et al., 2009); (ii) 2-APB (an activator of TRPV3 we used in our current studies) activates keratinocytes from DS-Nh mice at lower concentrations than control keratinocytes; (iii) TRPV3 activation leads to TSLP secretion in DS-Nh mice using TRPV3-KO mice as control (Yamamoto-Kasai et al., 2013). TRPV3 expression has also been shown to be increased in keratinocytes of atopic dermatitis (hence most probably inflamed) lesions (Yamamoto-Kasai et al. 2013). In support of these findings we also identified TRPV3 expression in human epidermis, as well as on cultured primary human keratinocytes, both on the mRNA and protein levels (Figure 1). Our results further show that TRPV3 is functional on keratinocytes and acts as a calcium-permeable channel (Figure 2), similarly to results on other cells types (Borbíró et al. 2011; Lee et al. 2016; Morgan et al. 2013; Pires et al. 2015; Somogyi et al. 2015), and in murine keratinocytes (Chung et al. 2004b; Huang et al. 2008; Mandadi et al. 2009). Since the calcium increase was abrogated in the absence of extracellular calcium, it is likely that TRPV3 acts as a membrane channel. Of great importance this is the first report in the literature that shows that TRPV3 natively expressed on primary human epidermal keratinocytes is a functionally active membrane channel. Activation of the channel with carvacrol or 2-APB elicited not only an increase in intracellular calcium as stated above, but also decreased the viability and proliferation of the cells, through the induction of apoptosis.

Although both activators used are considered non-selective - carvacrol has been shown to activate TRPA1 (Xu et al. 2006) while 2-APB activates TRPV1 and TRPV2 (Colton and Zhu 2007) - RNAi-mediated knockdown of TRPV3 significantly blocked all observed effects which suggests they were all (at least dominantly) TRPV3-dependent. Collectively these data coincide well with previous results on human hair follicles (Borbíró et al. 2011), where TRPV3 has been shown to induce apoptosis and catagen regression, and similar effects described by us on outer root sheath keratinocytes.

TRPV3 agonists also induced production and release of pro-inflammatory mediators from keratinocytes (Figure 4a-d). Inflammatory mediator production by keratinocytes is well-documented (Gröne 2002; Karsak et al. 2007; Oláh et al. 2016), and links the epidermis to the generally immunologically more active dermal compartment.

The role of epidermal TRPV3 in intercellular communication has been demonstrated in murine skin (Mandadi et al. 2009), where an increase in temperature resulted in ATP release from keratinocytes and subsequent activation of nerve endings. Our results expand the downstream targets of epidermal TRPV3 to immune cells, and hint at one of the possible mechanisms by which gain-of-function TRPV3 mutations may lead to skin lesions and pruritus, both of which are characteristics found in DS-Nh mice and patients suffering from Olmsted syndrome (Agarwala et al. 2016; Asakawa et al. 2006; Duchatelet et al. 2014; Lai-Cheong et al. 2012; Lin et al. 2012; Yoshioka et al. 2009). Recent research has also shown increased epidermal TRPV3 expression in atopic dermatitis (Yamamoto-Kasai et al. 2013) and patients suffering post-burn pruritus (Yang et al. 2015). The induction of pro-inflammatory mediator production was dependent on NF- κ B activation and translocation, which has been shown to be pivotal in several pro-inflammatory pathways on keratinocytes, for example in hypertrophic scar tissue through TRPC3 activation (Ishise et al. 2015), in UVB

induced inflammation (Ali et al. 2016; Ali and Sultana 2012), and TGF β 1 signaling (Tobar et al. 2010).

Although the clinical symptoms and murine phenotype associated with TRPV3 gain-of-function mutations unequivocally argue that the channel plays a central role in cutaneous homeostasis, there is currently no study investigating the human channel on the molecular level. This is the specific lack our results address. Collectively, our data shows for the first time that TRPV3 is functionally expressed on human epidermal keratinocytes and their activation decreases cell viability and induces pro-inflammatory mediator production through NF- κ B. Moreover, our exciting data invite further (both pre-clinical and clinical) studies to uncover the therapeutic potential of TRPV3-targeting pharmacological tools (most preferably which induce the inhibition and/or down-regulation of the ion channel) in the management of inflammatory skin conditions such as e.g. atopic dermatitis or other dermatitis types induced by allergens, irritants or other stimuli.

MATERIALS AND METHODS

Materials

Carvacrol and 2-aminoethoxydiphenyl borate (2-APB) were purchased from Sigma-Aldrich (St Louis, MO). Both were dissolved into dimethyl sulfoxide, also from Sigma-Aldrich. Vehicle control contained only the solvent at the same ratio as the treated group (1:1000).

Cell culturing

Human skin samples were obtained following written informed consent from healthy individuals undergoing dermatosurgery, adhering to Helsinki guidelines, and after obtaining Institutional Research Ethics Committee's and Government Office for Hajdú-Bihar County's permission (protocol No.: DE OEC RKEB/IKEB 3721-2012; document No). A detailed

description of culturing conditions may be found in the supplementary Materials and Methods. All experiments were performed on at least three independent donors.

Immunohistochemistry

Paraffin-embedded sections (5 μm), after antigen retrieval (in citrate-buffer, pH 6.0, at 750 W in microwave oven for 10 min), were first incubated with primary goat antibody against human TRPV3 (cat. No.-: NBP1-46342 Novus Biologicals LLC, Littleton, CO, USA). After staining with the primary antibodies, sections were incubated with biotinylated anti-goat IgG (1:200) (Bio-Rad, Hercules, CA, USA) for TRPV3. Immunoreactions were visualized using DAB reagent (DAKO, Golstrup, Denmark) and the sections were counterstained by hematoxylin (Sigma-Aldrich). For negative controls of the labeling procedure, primary antibodies were omitted.

Immunocytochemistry

Cells were fixed in acetone, permeabilized by 0.1 % Triton X-100 (Sigma-Aldrich), and then incubated with primary antibodies against TRPV3 or p65 (1:200 and 1: 50 dilution, respectively Novus Biologicals). For fluorescence staining, slides were then incubated with FITC-conjugated secondary antibodies (dilution 1:1000) (Dobrosi et al. 2008; Tóth et al. 2009). Nuclear counterstaining was performed using 4'-6-diamidino-2-phenylindole (DAPI) in both protocols. Images were captured with a OLYMPUS Xcellence RT fluorescent microscope (Olympus, Tokyo, Japan).

Western blotting

Details of Western blotting may be found in the Supplementary Materials and Methods section.

RNA isolation, reverse transcription, quantitative “real-time” PCR (Q-PCR)

Q-PCR was performed on a Stratagene Mx3005P QPCR System (Agilent Technologies) by using the 5' nuclease assay. Total RNA was isolated using TRIzol (Life Technologies) according to the manufacturer's protocol, and the isolated RNA was quality-checked by Nanodrop-1000 Spectrophotometer (NanoDrop/Thermo Scientific). 1 µg of total RNA were then reverse-transcribed into cDNA by using the High Capacity cDNA Reverse Transcription Kit (Applied Biosystems) according to the manufacturer's protocol. PCR amplification was performed by using the TaqMan primers and probes (assay ID-s: Hs00376854_m1 for TRPV3, Hs00985639_m1 for IL-6, Hs00174103_m1 for IL-8, Hs00174092_m1 for IL-1 α , Hs00174128_m1 for TNF α) using the TaqMan universal PCR master mix protocol (Applied Biosystems). As internal controls, transcripts of glyceraldehyde 3-phosphate dehydrogenase (GAPDH), peptidyl-prolyl isomerase A (cyclophilin A; PPIA), and actin beta (ACTB) were determined (assay ID-s: Hs99999905_m1, Hs99999904_m1, and Hs99999903_m1, respectively). The amount of the transcripts was normalized to those of the relevant housekeeping gene using the Δ CT method.

Patch-clamp experiments

Details of patch clamp protocols and composition of solutions used can be found in the Supplementary Materials and Methods.

Fluorimetric FLIPR Ca²⁺-imaging

Ca²⁺-imaging was performed according to our previously optimized protocol. In brief, keratinocytes were seeded in 96-well black-well/clear-bottom plates (Greiner Bio-One) at a density of 10,000 cells per well. Cells were washed two times with 1% bovine serum albumin (Sigma-Aldrich) and 2.5 mM Probenecid (Sigma-Aldrich) containing Hank's solution (136.8 mM NaCl, 5.4 mM KCl, 0.34 mM Na₂HPO₄, 0.44 mM KH₂PO₄, 0.81 mM MgSO₄, 1.26 mM CaCl₂, 5.56 mM glucose, 4.17 mM NaHCO₃, pH 7.2, all from Sigma-Aldrich). The cells were

then incubated with 1 μ M Fluo-4 AM (Life Technologies) containing Hank's solution (100 μ l/well) at 37°C for 30 min, and were then washed three times with Hank's solution (100 μ l/well). The plates were then placed in a FLIPR (Molecular Devices), and changes in $[Ca^{2+}]_{ic}$ (reflected by changes fluorescence; excitation: 490 nm; emission: 520 nm) induced by various concentrations of the compounds were recorded in each well. Experiments were performed in quadruplicates and the averaged data (as well as SEM) were used in the calculations.

Determination of cellular viability

Cells were plated in 96-well plates (10,000 cells per well density) in quadruplicates and the number of viable cells was determined by measuring the conversion of the tetrazolium salt MTT (3-(4,5-dimethylthiazol-2-yl)-2,5-diphenyltetrazolium bromide; Sigma-Aldrich) to formazan by mitochondrial dehydrogenases.

Determination of cellular proliferation

The degree of cellular growth (reflecting number of viable cells) was determined by measuring the DNA content of cells using CyQUANT Cell Proliferation Assay Kit (Invitrogen). Keratinocytes (10,000 cells per well) were cultured in 96-well black-well/clear-bottom plates (Greiner Bio-One) in quadruplicates and were treated with various concentrations of TRPV3 agonists. Supernatants were then removed by blotting on paper towels, and the plates were subsequently frozen at -70°C. The plates were then thawed at room temperature, and 200 μ l of CyQUANT dye/cell lysis buffer mixture was added to each well. After 5 minutes of incubation, fluorescence was measured at 490 nm excitation and 520 nm emission wavelengths using FLIPR (Molecular Devices).

RNA interference

Cells were transfected at $\approx 70\%$ confluence with specific Stealth RNAi oligonucleotides (40 nM, Invitrogen) against TRPV3 channels (ID-s: HSS136315, HSS136316, and HSS175965), using Lipofectamine 2000 Transfection Reagent (Invitrogen). For controls, RNAi Negative Control Duplexes (scrambled RNAi; Invitrogen) were employed. The 3 sequences supplied by the manufacturer were applied separately. The efficacy of RNAi-driven “knockdown” was evaluated after transfection by Western blotting as described previously above. Optical density was normalized to β -actin (antibody from Sigma-Aldrich, applied in 1:1000 dilution) and expressed relative to cells transfected with scrambled RNAi. In each case, the most effective RNAi oligonucleotide was selected and then used in subsequent functional experiments.

Determination of cytokine release (ELISA)

Samples of media were collected from keratinocyte cells exposed to different treatment. The supernatants were analyzed for human cytokines using commercially available ELISA kits (IL-6 and IL-8, BD Biosciences) according to the manufacturer’s protocols. In brief, plates were coated with Capture Antibody diluted in Coating Buffer (0.1 M Sodium Carbonate, pH 9.5 with 10 N NaOH; Sigma-Aldrich) and incubated overnight at 4°C. Plates were incubated with Assay Diluent [10% fetal bovine serum, Life Technologies in Phosphate-Buffered Saline (PBS: 80.0g NaCl, 11.6g Na₂HPO₄, 2.0g KH₂PO₄, 2.0g KCL, dH₂O to 10 L, all from Sigma-Aldrich) pH 7.0] at room temperature (RT) for 1 hour, while standard and sample dilutions were prepared in Assay Diluent. Standard and samples were added into appropriate wells and incubated for 2 hrs at RT. After 2 hours, Working Detector (Detection Antibody + SAV-HRP reagent) was added to each well, and incubated 1 hour at RT. After every each steps, plates were washed with Wash Buffer (0.05% Tween-20, Sigma-Aldrich in PBS). After washing, Substrate Solution [Tetramethylbenzidine (TMB), Sigma-Aldrich; and Hydrogen Peroxide in citrate-buffer, pH 5.0] was added to each well for 30 minutes in the dark, followed by Stop

Solution (2 N H₂SO₄). Absorbance was read at 450 nm or 405 nm within 30 minutes of stopping reaction. The amount of cytokines in pg/ml was calculated from standard curve. The experiments were repeated 3 times using different medium solutions.

CONFLICT OF INTEREST

The authors state no conflict of interest.

ACKNOWLEDGEMENTS

This work was supported by Hungarian reseach grants (OTKA 105369, NKFIH K120552, NKFIH K120187 GINOP-2.3.2-15-2016-00015) and a financial support from Ono Pharmaceutical Co., Ltd.

REFERENCES

- Agarwala MK, George R, Pramanik R, McGrath JA. Olmsted syndrome in an Indian male with a new de novo mutation in TRPV3. *Br. J. Dermatol.* 2016;174(1):209–11
- Ali F, Khan BA, Sultana S. Wedelolactone mitigates UVB induced oxidative stress, inflammation and early tumor promotion events in murine skin: plausible role of NFkB pathway. *Eur. J. Pharmacol.* 2016;786:253–64
- Ali F, Sultana S. Repeated short-term stress synergizes the ROS signalling through up regulation of NFkB and iNOS expression induced due to combined exposure of trichloroethylene and UVB rays. *Mol. Cell. Biochem.* 2012;360(1–2):133–45
- Asakawa M, Yoshioka T, Matsutani T, Hikita I, Suzuki M, Oshima I, et al. Association of a mutation in TRPV3 with defective hair growth in rodents. *J. Invest. Dermatol.* 2006;126(12):2664–72
- Atoyan R, Shander D, Botchkareva NV. Non-neuronal expression of transient receptor potential type A1 (TRPA1) in human skin. *J. Invest. Dermatol.* 2009;129(9):2312–5
- Barrett T, Wilhite SE, Ledoux P, Evangelista C, Kim IF, Tomashevsky M, et al. NCBI GEO: archive for functional genomics data sets—update. *Nucleic Acids Res.* 2013;41(D1):D991–5
- Beck B, Lehen'kyi V, Roudbaraki M, Flourakis M, Charveron M, Bordat P, et al. TRPC channels determine human keratinocyte differentiation: new insight into basal cell carcinoma. *Cell Calcium.* 2008;43(5):492–505
- Bíró T, Tóth BI, Marincsák R, Dobrosi N, Géczy T, Paus R. TRP channels as novel players in the pathogenesis and therapy of itch. *Biochim. Biophys. Acta.* 2007;1772(8):1004–21
- Bodó E, Bíró T, Telek A, Czifra G, Griger Z, Tóth BI, et al. A hot new twist to hair biology: involvement of vanilloid receptor-1 (VR1/TRPV1) signaling in human hair growth control. *Am. J. Pathol.* 2005;166(4):985–98

- Borbíró I, Lisztes E, Tóth BI, Czifra G, Oláh A, Szöllosi AG, et al. Activation of transient receptor potential vanilloid-3 inhibits human hair growth. *J. Invest. Dermatol.* 2011;131(8):1605–14
- Cheng X, Jin J, Hu L, Shen D, Dong X-P, Samie MA, et al. TRP channel regulates EGFR signaling in hair morphogenesis and skin barrier formation. *Cell.* 2010;141(2):331–43
- Chung M-K, Lee H, Mizuno A, Suzuki M, Caterina MJ. 2-aminoethoxydiphenyl borate activates and sensitizes the heat-gated ion channel TRPV3. *J. Neurosci. Off. J. Soc. Neurosci.* 2004a;24(22):5177–82
- Chung M-K, Lee H, Mizuno A, Suzuki M, Caterina MJ. TRPV3 and TRPV4 mediate warmth-evoked currents in primary mouse keratinocytes. *J. Biol. Chem.* 2004b;279(20):21569–75
- Colton CK, Zhu MX. 2-Aminoethoxydiphenyl borate as a common activator of TRPV1, TRPV2, and TRPV3 channels. *Handb. Exp. Pharmacol.* 2007;(179):173–87
- Danso-Abeam D, Zhang J, Dooley J, Staats KA, Van Eyck L, Van Brussel T, et al. Olmsted syndrome: exploration of the immunological phenotype. *Orphanet J. Rare Dis.* 2013;8:79
- Denda M, Sokabe T, Fukumi-Tominaga T, Tominaga M. Effects of skin surface temperature on epidermal permeability barrier homeostasis. *J. Invest. Dermatol.* 2007;127(3):654–9
- Denda M, Tsutsumi M, Denda S. Topical application of TRPM8 agonists accelerates skin permeability barrier recovery and reduces epidermal proliferation induced by barrier insult: role of cold-sensitive TRP receptors in epidermal permeability barrier homeostasis. *Exp. Dermatol.* 2010;19(9):791–5
- Devi S, Kedlaya R, Maddodi N, Bhat KMR, Weber CS, Valdivia H, et al. Calcium homeostasis in human melanocytes: role of transient receptor potential melastatin 1

- (TRPM1) and its regulation by ultraviolet light. *Am. J. Physiol. Cell Physiol.* 2009;297(3):C679-687
- Dobrosi N, Tóth BI, Nagy G, Dózsa A, Géczy T, Nagy L, et al. Endocannabinoids enhance lipid synthesis and apoptosis of human sebocytes via cannabinoid receptor-2-mediated signaling. *FASEB J. Off. Publ. Fed. Am. Soc. Exp. Biol.* 2008;22(10):3685–95
- Duchatelet S, Guibbal L, de Veer S, Fraitag S, Nitschké P, Zarhrate M, et al. Olmsted syndrome with erythromelalgia caused by recessive transient receptor potential vanilloid 3 mutations. *Br. J. Dermatol.* 2014;171(3):675–8
- Fernandes ES, Fernandes MA, Keeble JE. The functions of TRPA1 and TRPV1: moving away from sensory nerves. *Br. J. Pharmacol.* 2012;166(2):510–21
- Gröne A. Keratinocytes and cytokines. *Vet. Immunol. Immunopathol.* 2002;88(1–2):1–12
- Huang SM, Lee H, Chung M-K, Park U, Yu YY, Bradshaw HB, et al. Overexpressed transient receptor potential vanilloid 3 ion channels in skin keratinocytes modulate pain sensitivity via prostaglandin E2. *J. Neurosci. Off. J. Soc. Neurosci.* 2008;28(51):13727–37
- Ishise H, Larson B, Hirata Y, Fujiwara T, Nishimoto S, Kubo T, et al. Hypertrophic scar contracture is mediated by the TRPC3 mechanical force transducer via NFκB activation. *Sci. Rep.* 2015;5:11620
- Karsak M, Gaffal E, Date R, Wang-Eckhardt L, Rehnelt J, Petrosino S, et al. Attenuation of allergic contact dermatitis through the endocannabinoid system. *Science.* 2007;316(5830):1494–7
- Lai-Cheong JE, Sethuraman G, Ramam M, Stone K, Simpson MA, McGrath JA. Recurrent heterozygous missense mutation, p.Gly573Ser, in the TRPV3 gene in an Indian boy with sporadic Olmsted syndrome. *Br. J. Dermatol.* 2012;167(2):440–2

- Lee HC, Yoon S-Y, Lykke-Hartmann K, Fissore RA, Carvacho I. TRPV3 channels mediate Ca^{2+} influx induced by 2-APB in mouse eggs. *Cell Calcium*. 2016;59(1):21–31
- Lehen'kyi V, Beck B, Polakowska R, Charveron M, Bordat P, Skryma R, et al. TRPV6 is a Ca^{2+} entry channel essential for Ca^{2+} -induced differentiation of human keratinocytes. *J. Biol. Chem*. 2007;282(31):22582–91
- Lehen'kyi V, Vandenberghe M, Belaubre F, Julié S, Castex-Rizzi N, Skryma R, et al. Acceleration of keratinocyte differentiation by transient receptor potential vanilloid (TRPV6) channel activation. *J. Eur. Acad. Dermatol. Venereol. JEADV*. 2011;25 Suppl 1:12–8
- Lin Z, Chen Q, Lee M, Cao X, Zhang J, Ma D, et al. Exome sequencing reveals mutations in TRPV3 as a cause of Olmsted syndrome. *Am. J. Hum. Genet*. 2012;90(3):558–64
- Mandadi S, Sokabe T, Shibasaki K, Katanosaka K, Mizuno A, Moqrich A, et al. TRPV3 in keratinocytes transmits temperature information to sensory neurons via ATP. *Pflug. Arch. Eur. J. Physiol*. 2009;458(6):1093–102
- Moran MM, McAlexander MA, Bíró T, Szallasi A. Transient receptor potential channels as therapeutic targets. *Nat. Rev. Drug Discov*. 2011;10(8):601–20
- Morgan PJ, Hübner R, Rolfs A, Frech MJ. Spontaneous calcium transients in human neural progenitor cells mediated by transient receptor potential channels. *Stem Cells Dev*. 2013;22(18):2477–86
- Nair RP, Duffin KC, Helms C, Ding J, Stuart PE, Goldgar D, et al. Genome-wide scan reveals association of psoriasis with IL-23 and NF-kappaB pathways. *Nat. Genet*. 2009;41(2):199–204
- Nilius B, Appendino G. Spices: the savory and beneficial science of pungency. *Rev. Physiol. Biochem. Pharmacol*. 2013;164:1–76

- Nilius B, Owsianik G. The transient receptor potential family of ion channels. *Genome Biol.* 2011;12(3):218
- Oancea E, Vriens J, Brauchi S, Jun J, Splawski I, Clapham DE. TRPM1 forms ion channels associated with melanin content in melanocytes. *Sci. Signal.* 2009;2(70):ra21
- Oberwinkler J, Philipp SE. TRPM3. *Handb. Exp. Pharmacol.* 2014;222:427–59
- Oláh A, Ambrus L, Nicolussi S, Gertsch J, Tubak V, Kemény L, et al. Inhibition of fatty acid amide hydrolase exerts cutaneous anti-inflammatory effects both in vitro and in vivo. *Exp. Dermatol.* 2016;25(4):328–30
- Oláh A, Tóth BI, Borbíró I, Sugawara K, Szöllösi AG, Czifra G, et al. Cannabidiol exerts sebostatic and antiinflammatory effects on human sebocytes. *J. Clin. Invest.* 2014;124(9):3713–24
- Peier AM, Reeve AJ, Andersson DA, Moqrich A, Earley TJ, Hergarden AC, et al. A heat-sensitive TRP channel expressed in keratinocytes. *Science.* 2002;296(5575):2046–9
- Pires PW, Sullivan MN, Pritchard HAT, Robinson JJ, Earley S. Unitary TRPV3 channel Ca^{2+} influx events elicit endothelium-dependent dilation of cerebral parenchymal arterioles. *Am. J. Physiol. Heart Circ. Physiol.* 2015;309(12):H2031-2041
- Qin J-Z, Chaturvedi V, Denning MF, Choubey D, Diaz MO, Nickoloff BJ. Role of NF- κ B in the Apoptotic-resistant Phenotype of Keratinocytes. *J. Biol. Chem.* 1999;274(53):37957–64
- Saito S, Shingai R. Evolution of thermoTRP ion channel homologs in vertebrates. *Physiol. Genomics.* 2006;27(3):219–30
- Somogyi CS, Matta C, Foldvari Z, Juhász T, Katona É, Takács ÁR, et al. Polymodal Transient Receptor Potential Vanilloid (TRPV) Ion Channels in Chondrogenic Cells. *Int. J. Mol. Sci.* 2015;16(8):18412–38

- Sulk M, Seeliger S, Aubert J, Schwab VD, Cevikbas F, Rivier M, et al. Distribution and Expression of Non-Neuronal Transient Receptor Potential (TRPV) Ion Channels in Rosacea. *J. Invest. Dermatol.* 2012;132(4):1253–62
- Szöllősi AG, Oláh A, Tóth IB, Papp F, Czifra G, Panyi G, et al. Transient receptor potential vanilloid-2 mediates the effects of transient heat shock on endocytosis of human monocyte-derived dendritic cells. *FEBS Lett.* 2013;587(9):1440–5
- Takai T, Chen X, Xie Y, Vu AT, Le TA, Kinoshita H, et al. TSLP expression induced via Toll-like receptor pathways in human keratinocytes. *Methods Enzymol.* 2014;535:371–87
- Tobar N, Villar V, Santibanez JF. ROS-NFkappaB mediates TGF-beta1-induced expression of urokinase-type plasminogen activator, matrix metalloproteinase-9 and cell invasion. *Mol. Cell. Biochem.* 2010;340(1–2):195–202
- Tóth BI, Benko S, Szöllosi AG, Kovács L, Rajnavölgyi E, Bíró T. Transient receptor potential vanilloid-1 signaling inhibits differentiation and activation of human dendritic cells. *FEBS Lett.* 2009;583(10):1619–24
- Tóth BI, Dobrosi N, Dajnoki A, Czifra G, Oláh A, Szöllosi AG, et al. Endocannabinoids modulate human epidermal keratinocyte proliferation and survival via the sequential engagement of cannabinoid receptor-1 and transient receptor potential vanilloid-1. *J. Invest. Dermatol.* 2011;131(5):1095–104
- Vay L, Gu C, McNaughton PA. The thermo-TRP ion channel family: properties and therapeutic implications. *Br. J. Pharmacol.* 2012;165(4):787–801
- Wu L-J, Sweet T-B, Clapham DE. International Union of Basic and Clinical Pharmacology. LXXVI. Current progress in the mammalian TRP ion channel family. *Pharmacol. Rev.* 2010;62(3):381–404

- Wullaert A, Bonnet MC, Pasparakis M. NF- κ B in the regulation of epithelial homeostasis and inflammation. *Cell Res.* 2011;21(1):146–58
- Xu H, Delling M, Jun JC, Clapham DE. Oregano, thyme and clove-derived flavors and skin sensitizers activate specific TRP channels. *Nat. Neurosci.* 2006;9(5):628–35
- Yamamoto-Kasai E, Yasui K, Shichijo M, Sakata T, Yoshioka T. Impact of TRPV3 on the development of allergic dermatitis as a dendritic cell modulator. *Exp. Dermatol.* 2013;22(12):820–4
- Yang YS, Cho SI, Choi MG, Choi YH, Kwak IS, Park CW, et al. Increased expression of three types of transient receptor potential channels (TRPA1, TRPV4 and TRPV3) in burn scars with post-burn pruritus. *Acta Derm. Venereol.* 2015;95(1):20–4
- Yoshioka T, Imura K, Asakawa M, Suzuki M, Oshima I, Hirasawa T, et al. Impact of the Gly573Ser substitution in TRPV3 on the development of allergic and pruritic dermatitis in mice. *J. Invest. Dermatol.* 2009;129(3):714–22

FIGURE LEGENDS

Figure 1. Transient receptor potential vanilloid-3 (TRPV3) is expressed in the epidermis of human skin and on cultured human epidermal keratinocytes (NHEK)

(a) TRPV3-specific immunoreactivity (IR), as revealed by EnVision technique, on human skin *in situ*. (b) Negative control of panel (a). (c) Immunofluorescence identification (FITC labeling, green fluorescence) of TRPV3 on primary cultures of NHEK keratinocytes. Nuclei were counterstained with 4'-6-diamidino-2-phenylindole (DAPI, blue fluorescence). (d) Negative control of panel (c). Scale bars mark (a-b) 100 μm and (c-d) 10 μm . (e) Western blot analysis. TRPV3 protein expression was determined on cell lysates of NHEK harvested at various confluences. PC2, 2 days at post-confluence. Equal loading was assessed by determining expression of β -actin. (f) Quantitative “real-time” PCR (Q-PCR) analysis of TRPV3 mRNA transcripts on human skin tissue and cell lysates of NHEK keratinocytes harvested at various confluences. PC2, 2 days at post-confluence. Data are expressed as mean \pm SEM of three independent determinations. Three additional experiments yielded similar results.

Figure 2. Transient receptor potential vanilloid-3 (TRPV3) is expressed as a Ca^{2+} -permeable ion channel on normal human epidermal keratinocytes (NHEK)

(a) Representative *I-V* curves recorded with a patch-clamp ramp protocol shown in the insets. (b) A usual time course of a single experiment showing 100 μM carvacrol-induced current values measured at -90 mV (open red symbols), at -40 mV (open green symbols), at $+40$ mV (open blue symbols), and at $+90$ mV (filled red symbols). (c) Statistical analysis of normalized currents to cell membrane capacitance (mean \pm SEM, $n=6$) measured at -40 mV (left side downward), $+40$ mV (left side upward), -90 mV (right side downward), and $+90$ mV (right side upward) in different conditions. (d, e) Representative fluorimetric Ca^{2+} -

imaging data recorded on fluo-4-loaded NHEK keratinocytes. The arrow indicates the application of TRPV3 agonists carvacrol or 2-aminoethoxydiphenyl borate (2-APB) in different concentrations in solutions containing normal (1.8 mM) $[Ca^{2+}]$. **(f)** Statistical analysis of maximal amplitudes of Ca^{2+} -elevations induced by the TRPV3 agonists in normal (1.8 mM) or low (0.02 mM) $[Ca^{2+}]$ solutions. In all cases, mean \pm SEM of multiple determinations ($n > 3$) is presented. For statistical analysis, # marks significant ($P < 0.05$) differences compared to the control, whereas * marks significant ($P < 0.05$) differences compared with the maximal TRPV3 activator-induced Ca^{2+} -elevations recorded in normal $[Ca^{2+}]$ solution.

Figure 3. Activation of transient receptor potential vanilloid-3 (TRPV3) on normal human epidermal keratinocytes (NHEK) decreases viability and inhibits proliferation

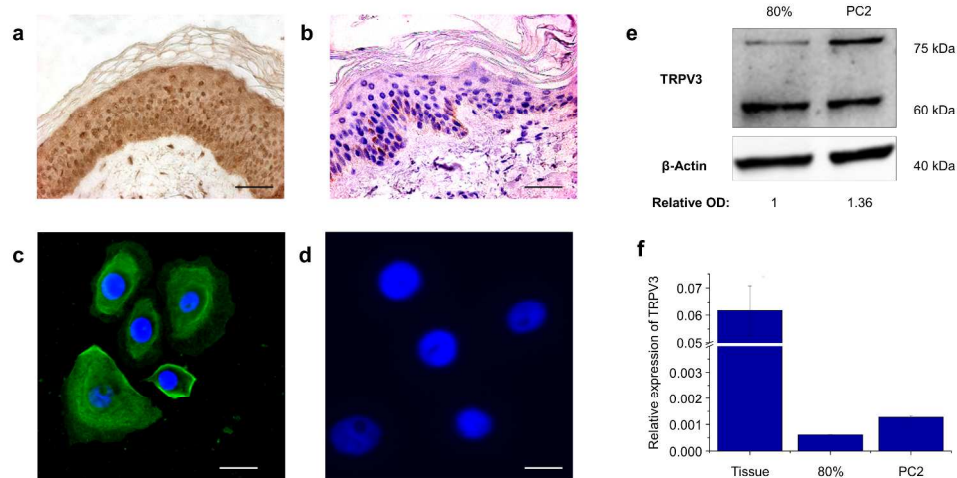
NHEK keratinocytes were treated with various concentrations of TRPV3 activators for 24 hours. **(a)** Determination of cell viability by colorimetric MTT (3-(4,5-dimethylthiazol-2-yl)-2,5-diphenyl tetrazolium bromide) cell viability assay. **(b)** Determination of proliferation by fluorimetric CyQuant assay. Data (mean \pm SEM) are expressed as a percentage of the mean value (defined as 100%) of the scrambled RNAi-non-treated group. For statistical analysis, * marks significant ($P < 0.05$) differences compared with the scrambled RNAi-non-treated group, whereas # marks significant ($P < 0.05$) differences compared with the equimolar TRPV3 activator (carvacrol or 2-APB) stimulated scrambled RNAi-treated group. Two additional experiments yielded similar results. 2-APB, 2-aminoethoxydiphenyl borate.

Figure 4. Activation of transient receptor potential vanilloid-3 (TRPV3) induces proinflammatory cytokine release on normal human epidermal keratinocytes (NHEK)

(a, b) Quantitative “real-time” PCR (Q-PCR) analysis of proinflammatory cytokines (IL-1 α , IL-6, IL-8, TNF α) after treating NHEK cells with TRPV3 activators 300 μ M carvacrol or 30

μM 2-aminoethoxydiphenyl borate (2-APB) for 3 hours. Data (mean \pm SEM) are normalized to the scrambled RNAi-non-treated group regarded as 1. **(c, d)** Determination of the released cytokine concentration following 6-hr and 12-hr treatments of NHEKs with 300 μM carvacrol. Data are presented as mean \pm SEM of three independent determinations. One additional experiment yielded similar results. For statistical analysis, * marks significant ($P < 0.05$) differences compared with the scrambled RNAi-non-treated group, whereas # marks significant ($P < 0.05$) differences compared with the TRPV3 activator stimulated scrambled RNAi-treated group. Two additional experiments yielded similar results. **(e)** Western blot analysis of lysates of NHEK cells treated with the TRPV3 activator 300 μM carvacrol, 60 μM of the calcium chelator EDTA, or their combinations for 30 minutes. Numbers on the OD row indicate the optical density of the P-I κ B α and P-P65 bands normalized to the corresponding β -actin signals. **(f-i)** immunofluorescent labelling of p65 in NHEK cells to show translocation of the protein to the nuclei. Cells were treated with 300 μM carvacrol, 60 μM EDTA, the combination of the two or 20 $\mu\text{g/ml}$ of polyinosinic:polycytidylic acid (poly I:C), a TLR3 activator used as a positive control for 30 minutes. Scale bars = 5 μm

Figure 1.

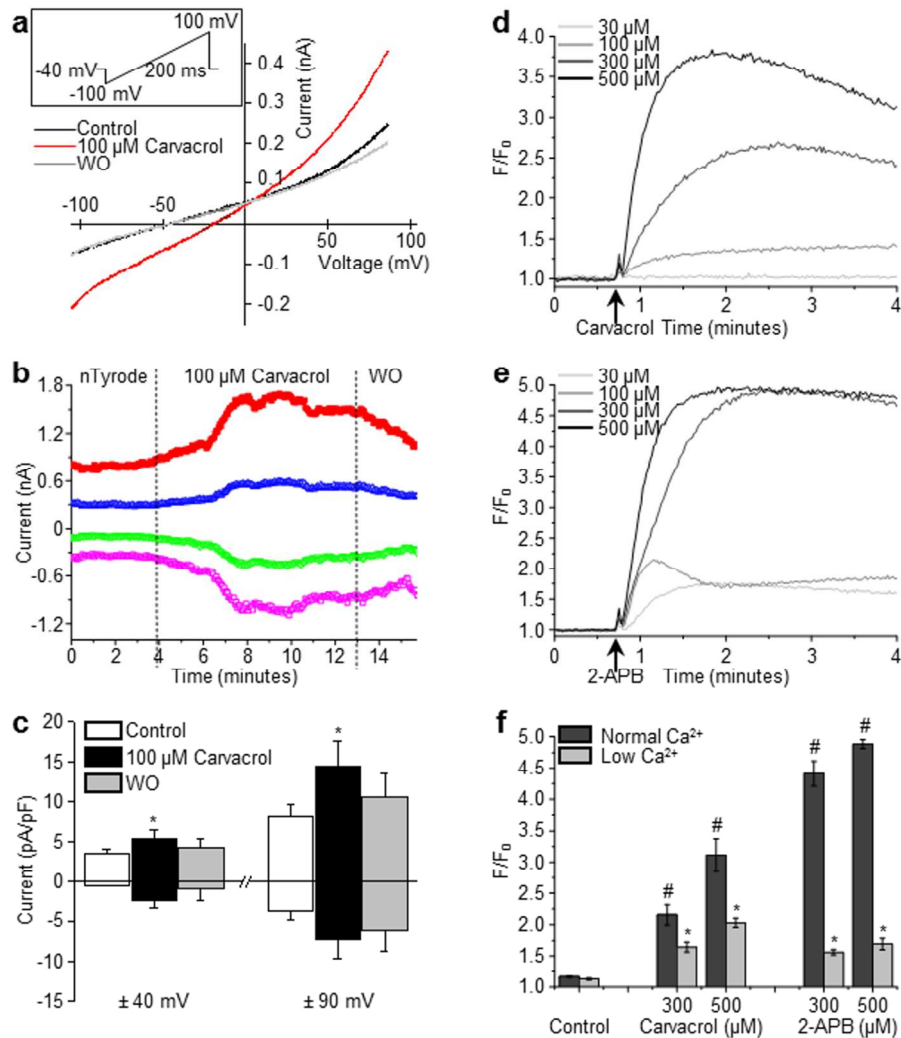


Transient receptor potential vanilloid-3 (TRPV3) is expressed in the epidermis of human skin and on cultured human epidermal keratinocytes (NHEK)

(a) TRPV3-specific immunoreactivity (IR), as revealed by EnVision technique, on human skin in situ. (b) Negative control of panel (a). (c) Immunofluorescence identification (FITC labeling, green fluorescence) of TRPV3 on primary cultures of NHEK keratinocytes. Nuclei were counterstained with 4'-6-diamidino-2-phenylindole (DAPI, blue fluorescence). (d) Negative control of panel (c). Scale bars mark (a-b) 100 μ m and (c-d) 10 μ m. (e) Western blot analysis. TRPV3 protein expression was determined on cell lysates of NHEK harvested at various confluences. PC2, 2 days at post-confluence. Equal loading was assessed by determining expression of β -actin. (f) Quantitative "real-time" PCR (Q-PCR) analysis of TRPV3 mRNA transcripts on human skin tissue and cell lysates of NHEK keratinocytes harvested at various confluences. PC2, 2 days at post-confluence. Data are expressed as mean \pm SEM of three independent determinations. Three additional experiments yielded similar results.

323x183mm (300 x 300 DPI)

Figure 2.



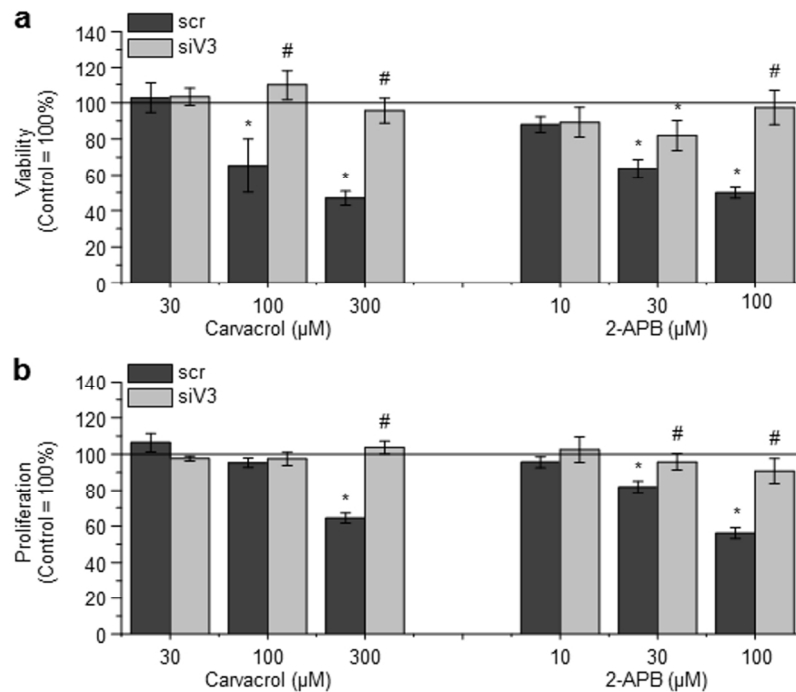
Transient receptor potential vanilloid-3 (TRPV3) is expressed as a Ca²⁺-permeable ion channel on normal human epidermal keratinocytes (NHEK)

(a) Representative I-V curves recorded with a patch-clamp ramp protocol shown in the insets. (b) A usual time course of a single experiment showing 100 μM carvacrol-induced current values measured at -90 mV (open red symbols), at -40 mV (open green symbols), at +40 mV (open blue symbols), and at +90 mV (filled red symbols). (c) Statistical analysis of normalized currents to cell membrane capacitance (mean ± SEM, n=6) measured at -40 mV (left side downward), +40 mV (left side upward), -90 mV (right side downward), and +90 mV (right side upward) in different conditions. (d, e) Representative fluorimetric Ca²⁺-imaging data recorded on fluo-4-loaded NHEK keratinocytes. The arrow indicates the application of TRPV3 agonists carvacrol or 2-aminoethoxydiphenyl borate (2-APB) in different concentrations in solutions containing normal (1.8 mM) [Ca²⁺]. (f) Statistical analysis of maximal amplitudes of Ca²⁺-elevations induced by the TRPV3 agonists in normal (1.8 mM) or low (0.02 mM) [Ca²⁺] solutions. In all cases, mean ± SEM of multiple determinations (n > 3) is presented. For statistical analysis, # marks significant (P < 0.05)

differences compared to the control, whereas * marks significant ($P < 0.05$) differences compared with the maximal TRPV3 activator-induced Ca^{2+} -elevations recorded in normal $[\text{Ca}^{2+}]$ solution.

112x135mm (300 x 300 DPI)

Figure 3.

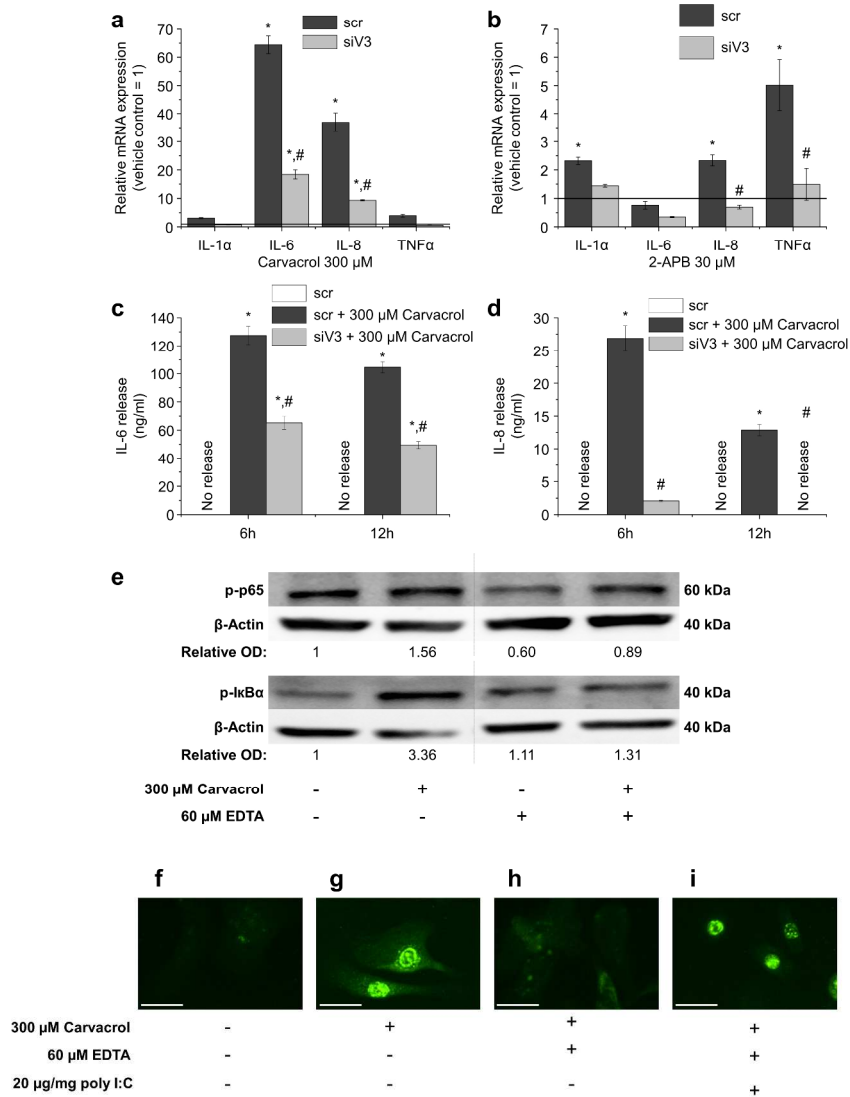


Activation of transient receptor potential vanilloid-3 (TRPV3) on normal human epidermal keratinocytes (NHEK) decreases viability and inhibits proliferation

NHEK keratinocytes were treated with various concentrations of TRPV3 activators for 24 hours. (a) Determination of cell viability by colorimetric MTT (3-(4,5-dimethylthiazol-2-yl)-2,5-diphenyl tetrazolium bromide) cell viability assay. (b) Determination of proliferation by fluorimetric CyQuant assay. Data (mean \pm SEM) are expressed as a percentage of the mean value (defined as 100%) of the scrambled RNAi-non-treated group. For statistical analysis, * marks significant ($P < 0.05$) differences compared with the scrambled RNAi-non-treated group, whereas # marks significant ($P < 0.05$) differences compared with the equimolar TRPV3 activator (carvacrol or 2-APB) stimulated scrambled RNAi-treated group. Two additional experiments yielded similar results. 2-APB, 2-aminoethoxydiphenyl borate.

111x93mm (300 x 300 DPI)

Figure 4.



Activation of transient receptor potential vanilloid-3 (TRPV3) induces proinflammatory cytokine release on normal human epidermal keratinocytes (NHEK)

(a, b) Quantitative "real-time" PCR (Q-PCR) analysis of proinflammatory cytokines (IL-1 α , IL-6, IL-8, TNF α) after treating NHEK cells with TRPV3 activators 300 μ M carvacrol or 30 μ M 2-aminoethoxydiphenyl borate (2-APB) for 3 hours. Data (mean \pm SEM) are normalized to the scrambled RNAi-non-treated group regarded as 1. (c, d) Determination of the released cytokine concentration following 6-hr and 12-hr treatments of NHEKs with 300 μ M carvacrol. Data are presented as mean \pm SEM of three independent determinations.

One additional experiment yielded similar results. For statistical analysis, * marks significant ($P < 0.05$) differences compared with the scrambled RNAi-non-treated group, whereas # marks significant ($P < 0.05$) differences compared with the TRPV3 activator stimulated scrambled RNAi-treated group. Two additional experiments yielded similar results. (e) Western blot analysis of lysates of NHEK cells treated with the TRPV3 activator 300 μ M carvacrol, 60 μ M of the calcium chelator EDTA, or their combinations for 30 minutes. Numbers on the OD row indicate the optical density of the P-I κ B α and P-P65 bands normalized to

the corresponding β -actin signals. (f-i) immunofluorescent labelling of p65 in NHEK cells to show translocation of the protein to the nuclei. Cells were treated with 300 μ M carvacrol, 60 μ M EDTA, the combination of the two or 20 μ g/ml of polyinosinic:polycytidylic acid (poly I:C), a TLR3 activator used as a positive control for 30 minutes. Scale bars = 5 μ m

1108x1460mm (72 x 72 DPI)

SUPPLEMENTARY MATERIAL

Supplementary Materials and Methods

Cell culturing

Epidermal sheets were cut into 3-5 mm² squares; keratinocytes were isolated after overnight dermo-epidermal separation in 2.4 U ml⁻¹ dispase (Sigma-Aldrich) by short trypsin (0.05%, Sigma-Aldrich) digestion. Trypsin was deactivated by addition of 5x volume of DMEM supplemented with 10% FBS and penicillin/streptomycin (all from Life Technologies, Carlsbad, CA). Cells were cultured for the first two days in DMEM/HAM F12 medium (mixed in a 3:1 ratio) supplemented with insulin, hydrocortisone, adenine, T3, cholera toxin, EGF, ascorbyl-2-phosphate, penicillin G (all from Sigma-Aldrich), gentamycin (Life Technologies) and Fetal Clone II serum equivalent (Hyclone, South Logan, UT, USA) to make sure the cells attach. Once cells have attached (3-5 days, depending on the donor) the cells are cultured in EpiLife serum-free media supplemented with Human Keratinocyte Growth Supplement (all from Life Technologies). Medium was changed every other day and cells are passaged at ≈80% confluence.

Western blotting

Cells were harvested and homogenized in detergent mixture (50mM TRIS HCl, 150 mM NaCl, 1% Triton X-100, 1% Igepal CA 630, 0.5% sodium deoxycholate; Sigma-Aldrich), containing protease inhibitor cocktail (1:100; Sigma-Aldrich). After sonication the protein content of the resulting samples was determined by a modified BCA protein assay (Pierce). Protein samples (1 µg/well) were subjected to SDS-PAGE (10% Mini Protean TGX gels, BioRad), and transferred to nitrocellulose membranes, by using Trans-Blot® Turbo™ Nitrocellulose Transfer Packs and Trans Blot Turbo System (both from BioRad). Membranes were probed with the corresponding primary antibodies against human TRPV3 (1:500 dilution, NOVUS Biologicals), **IκBα**, **p65** in 5% milk containing PBS) overnight at 4°C. As a secondary antibody horseradish peroxidase-conjugated goat-anti-rabbit or mouse IgG antibodies were used (1:1000, Bio-Rad) and the immunoreactive bands were visualized by a SuperSignal West Pico Chemiluminescent Substrate-Enhanced Chemiluminescence kit (Pierce, Rockford, IL, United States) using LAS-3000 Intelligent Dark

Box (Fuji, Tokyo, Japan) Gel Logic 1500 Imaging System (Kodak, Tokyo, Japan). To assess equal loading, the membranes were re-probed by using rabbit-anti- β -actin antibodies (1:1000, Actin – A2668 (Sigma)). Densitometric analysis was performed by using ImageJ image analysis software (NIH, Bethesda, MA).

Patch-clamp experiments

Electrophysiological measurements were carried out on keratinocytes cultured in EpiLife serum-free media supplemented with Human Keratinocyte Growth Supplement (Life Technologies) on coverslips having 1 cm diameter. These coverslips (covered with NHEKs) were placed into a perfusion chamber mounted on a stage of an inverted microscope where the cells were continuously superfused with Tyrode's solution containing (in mM) NaCl 144, KCl 5.6, CaCl₂ 2.5, MgCl₂ 1.2, HEPES 5, glucose 10, at pH 7.4. The osmolarity of the solutions was carefully adjusted with a vapor pressure osmometer (Vapro 5520, Wescor Inc.). All experiments were performed at room temperature. Borosilicate glass pipettes were fabricated with a laser puller (Model P-2000, Sutter Instrument Company) having resistance of 2–4 M Ω after filling with pipette solution including (in mM) K-aspartate 100, KCl 45, MgCl₂ 1, HEPES 5, EGTA 10, K-ATP 3 at pH 7.2. TRPV3 currents were recorded with a Multiclamp-700B intracellular amplifier (Axon Instruments, Molecular Devices) using the whole cell configuration of the patch clamp technique. After establishing high (>1 G Ω) resistance seal by gentle suction, the cell membrane beneath the tip of the electrode was disrupted by further suction and/or by applying 1.5 V electrical pulses for 1 ms. Ion currents were normalized to cell capacitance, determined in each cell using short hyperpolarizing pulses from 10 mV to 20 mV. Outputs from the amplifier were digitized at 10 kHz using a Digidata-1440A A/D converter (Axon Instruments) under software control (pClamp 10.3, Axon Instruments). The series resistance was typically 6-10 M Ω and left uncompensated. Experiments were discarded when the series resistance was high or increased during the measurement or the amplitude of the current was unstable during the untreated control traces. Carvacrol (Sigma-Aldrich) was applied to the superfusate from a 1 M stock solution in dimethyl sulfoxide (DMSO, Sigma-Aldrich) reaching a final concentration of 100 μ M. The final concentration of DMSO was 0.1% since it has no effects on membrane currents. All values presented are arithmetic means \pm SEM.

Determination of necrosis

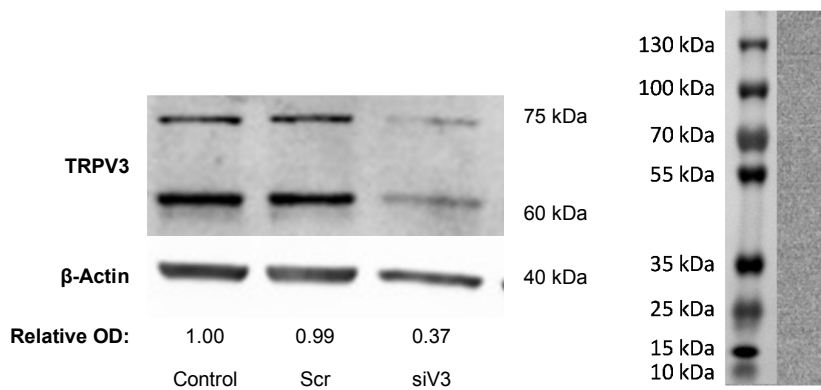
Quantification of cellular necrosis was based on the evaluation of plasma membrane fragmentation that allows SYTOX Green dye (Life Technologies) to penetrate cells and bind to nucleic acids. Cells were seeded (density: 10000 cells/well) in 96-well black-well/clear-bottom plates (Greiner Bio One), and octuplicates were treated with carvacrol and 2-APB with or without EDTA for 24 hours. After discarding supernatants, cells were incubated with 1 μ M SYTOX green dye for 30 minutes followed by a PBS wash. The fluorescence emission of SYTOX Green dye was monitored by a Flexstation III³⁸⁴ fluorescent plate reader at 545 nm excitation and 590 nm emission wavelengths.

Determination of apoptosis

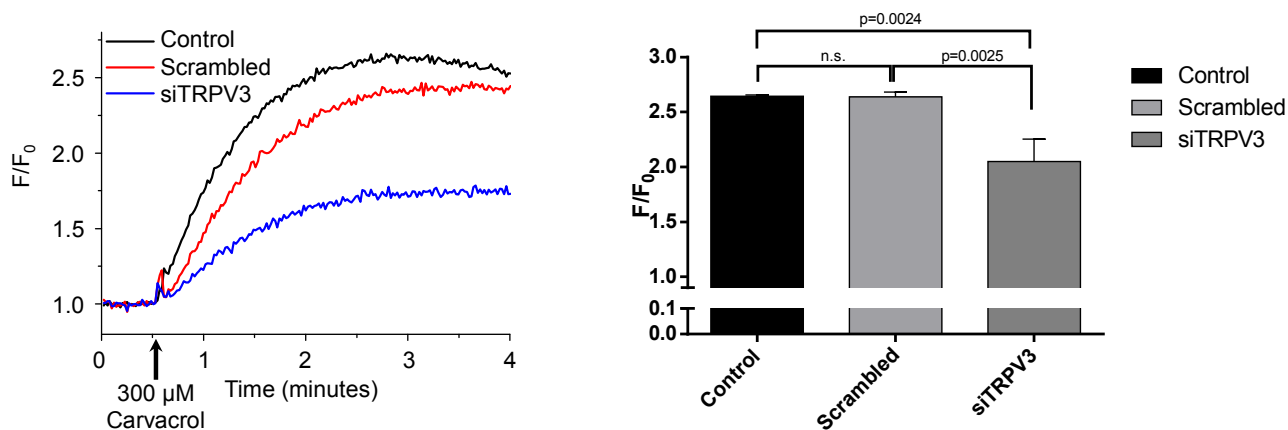
Apoptotic process was detected using MitoProbe DiIC1(5) Assay Kit (Life Technologies). The DiIC1(5) dye accumulates in the mitochondria dependent on the mitochondrial membrane potential, the decrease of which is an early sign of apoptosis. Cells were seeded (density: 10000 cells/well) in 96-well black-well/clear-bottom plates, and quadruplicates were treated with carvacrol and 2-APB with or without EDTA for 2 hours. After discarding supernatants, cells were incubated with DiIC1(5) solution for 30 minutes and the fluorescence of the dye was measured at 630 nm excitation and 670 nm emission wavelengths using a Flexstation III³⁸⁴ fluorescent plate reader

Statistical analysis

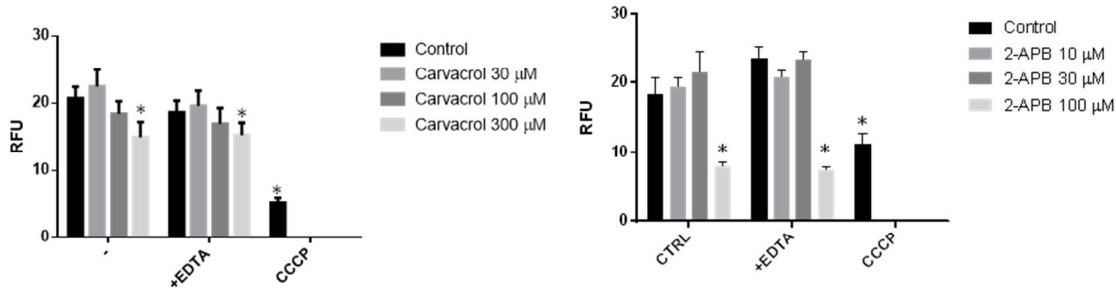
Data were analysed and graphs were plotted by Origin Pro Plus 6.0 (Microcal, Northampton, MA, USA), and Graphpad Prism software (Graphpad, San Diego, CA, USA) using ANOVA and $P < 0.05$ values were regarded as significant differences.

Supplementary results

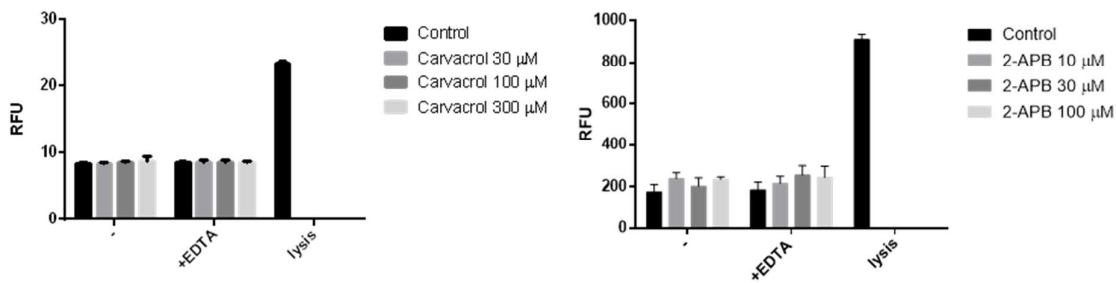
Supplementary Figure 1.: Western blot analysis of RNAi-mediated knockdown of TRPV3 on NHEKs, and an image of a negative staining using the same antibody (the protein sample tested was of monocyte-derived immature dendritic cells Szöllösi et al., 2013).



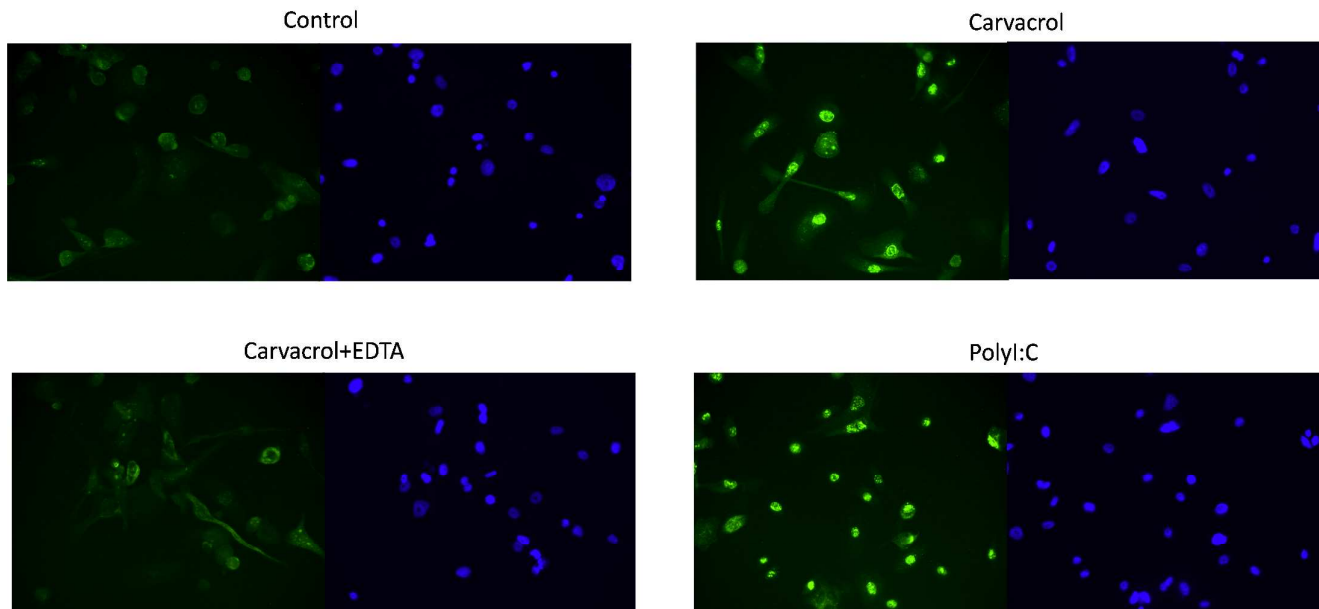
Supplementary Figure 2.: Representative fluorimetric Ca^{2+} recorded on fluo-4-loaded NHEKs. The arrow indicates the application of TRPV3 agonist carvacrol at 300 μM concentration. Statistical analysis of maximal amplitudes of Ca^{2+} -elevations induced by the TRPV3 agonist carvacrol on control, scrambled RNA and TRPV3 specific RNA transfected cells. In all cases, mean \pm SEM of multiple determinations ($n > 3$) is presented. Statistical significance is marked above relevant brackets between columns.



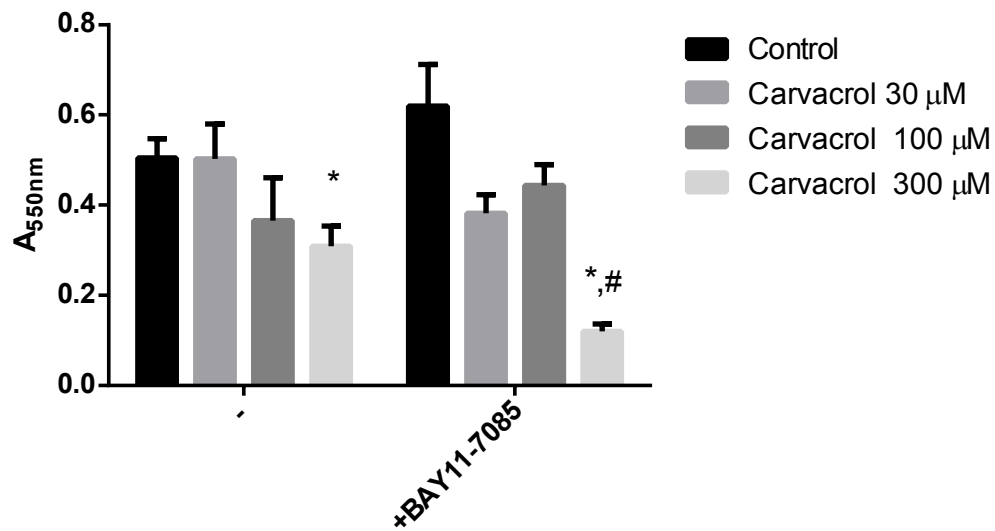
Supplementary Figure 3.: Activation of transient receptor potential vanilloid-3 (TRPV3) on normal human epidermal keratinocytes (NHEK) causes apoptosis: Evaluation of mitochondrial membrane potential using DiI(1)5 dye. Data (mean \pm SEM) are expressed in relative fluorescence units (RFU). * marks significant ($p < 0.05$) changes as compared to control, CCCP is a mitochondrial membrane potential disruptor used as a positive control. Two additional experiments yielded similar results. 2-APB, 2-aminoethoxydiphenyl borate.



Supplementary Figure 4.: Activation of transient receptor potential vanilloid-3 (TRPV3) on normal human epidermal keratinocytes (NHEK) does not causes necrosis. Evaluation of cellular necrosis using Sytox Green dye. Data (mean \pm SEM) are expressed in relative fluorescence units (RFU). Lysis buffer was used as a positive control for necrotic cell death. Two additional experiments yielded similar results. 2-APB, 2-aminoethoxydiphenyl borate.



Supplementary Figure 5.: TRPV3 activation causes translocation of p65 into the cell nuclei. Each image is juxtaposed with its nuclear counterstain (4'-6-diamidino-2-phenylindole [DAPI], blue fluorescence).



Supplementary Figure 6.: Inhibition of NF- κ B in parallel with TRPV3 activation further decreases viability on normal human epidermal keratinocytes (NHEK): Data (mean \pm SD) are expressed as a relative absorbance units. For statistical analysis, * marks significant ($P < 0.05$) differences compared with the control

group, whereas # marks significant ($P < 0.05$) differences compared with the equimolar TRPV3 activator stimulated, NF- κ B treated group. Two additional experiments yielded similar results.